

XAFS and neutron diffraction study of $\text{La}_{1-x}\text{Sr}_x\text{Co}_{1-y}\text{Nb}_y\text{O}_3$

V.V. Efimov^{a,*}, E. Efimova^a, D. Karpinsky^b, D.I. Kochubey^c, V. Kriventsov^c,
A. Kuzmin^d, S. Molodtsov^e, V. Sikolenko^{a,f}, J. Purans^g, S. Tiutiunnikov^a,
I.O. Troyanchuk^b, A.N. Shmakov^c, D. Vyalikh^e

^aJoint Institute for Nuclear Research, Joliot-Curie 6, Dubna 141980, Moscow Region, Russia

^bInstitute of Solid State and Semiconductor Physics, 220072 Minsk, Belarus

^cBorsovsk Institute of Catalysis, Lavrentiev prosp. 5, Novosibirsk 630090, Russia

^dInstitute of Solid State Physics, Kengaraga Str. 8, LV-1063 Riga, Latvia

^eInstitut für Kristallographie und Festkörperphysik (IKFP), Zellescher Weg 16, Physikgebäude C 115, 01069 Dresden, Germany

^fHahn-Meitner-Institut Glienicker Str. 100, Berlin D-14109, Germany

^gDipartimento di Fisica, Università di Trento, Via Sommarive 14, I-38050 Povo (Trento), Italy

Available online 21 January 2007

Abstract

The effect of hole doping on the crystal and electronic structure of $\text{La}_{1-x}\text{Sr}_x\text{Co}_{1-y}\text{Nb}_y\text{O}_3$ ($y = 0.0-0.25$) at the $x = 0.0; 0.2; 0.5$ has been studied by neutron diffraction and X-ray absorption spectroscopy at the Co K and $L_{2,3}$ -edges. The preliminary analysis of the Co K and $L_{2,3}$ -edges X-ray absorption near edge structure (XANES) in $\text{La}_{1-x}\text{Sr}_x\text{Co}_{1-y}\text{Nb}_y\text{O}_3$ series suggests that upon niobium doping, an increase of the intermediate Co^{3+} spin state and a decrease of low spin Co^{4+} states contributions occur. The possible explanation of the observed changes of crystal and electronic structure in these cobaltites is discussed.

© 2007 Elsevier B.V. All rights reserved.

PACS: 61.10.Ht; 61.12.Ld; 71.70.Ej; 75.25.+z; 75.30.Et; 76.30.Kg

Keywords: XAFS; X-ray and neutron diffraction; Cobaltites

1. Introduction

In LnCoO_3 oxides ($\text{Ln} \equiv$ lanthanide), Co ions in the ground state are characterized by the low-spin electronic configuration $t_{2g}^6 e_g^0$. This state (LS; $S = 0$) gradually passes to intermediate spin one (IS; $S = 1$; $t_{2g}^5 e_g^1$) with temperature enhancement [1]. For example, the spin state of cobalt ions in LaCoO_3 gradually changes from LS to IS with temperature increment in the temperature range of 40–100 K. In the case of $\text{La}_{1-x}\text{Sr}_x\text{CoO}_3$, the Sr^{2+} ionic radius is significantly greater than that of the La^{3+} ion; so it is possible to expect stabilization of the intermediate spin state of cobalt ions by substituting Sr^{2+} ions for La^{3+} ones [2]. However, at such heterovalent substitution low spin Co^{4+} ions appear [3], leading to the ferromagnetic metallic

ground state [4]. The majority of researchers suppose that ferromagnetism in cobaltites is caused by “a double exchange”, as in manganites. To prevent the Co^{4+} ion appearance, it is possible to introduce simultaneously Nb^{5+} ions, which at the presence of Co^{3+} ions will be in oxidizing state 5+. By simultaneously introducing Sr^{2+} and Nb^{5+} , the cobalt ions keep their valence state, and the electroconductivity of $\text{La}_{1-x}\text{Sr}_x\text{Co}_{1-y}\text{Nb}_y\text{O}_3$ solid solutions decreases with dopant concentration enhancement. Thus, the different nature of ferromagnetic interactions formation in the given systems is observed [5].

In the case of $\text{La}_{1-x}\text{Sr}_x\text{Co}_{1-x/2}\text{Nb}_{x/2}\text{O}_3$, the ferromagnetic component can be caused only by cobalt ions inside crystallites, as the average grain size is about 10 μm . We suppose that strontium ions, which have an ionic radius much larger than that of lanthanum ones, increase the mean Co–O distance in some CoO_6 octahedra, which favors the Co^{3+} ion transition from LS to IS state. Thus,

*Corresponding author. Tel.: +7 049621 64 173; fax: +7 49621 65 767.

E-mail address: efimov@sunse.jinr.ru (V.V. Efimov).

the nearest cobalt ions in IS state can interact ferromagnetically by means of the vibronic $e^1\text{--}O\text{--}e^0$ superexchange, but this coupling requires a dynamic Jahn–Teller distortion.

In this work, we present the results of neutron diffraction measurements and X-ray absorption near edge structure (XANES) at the Co K and $L_{2,3}$ -edges study of $\text{La}_{1-x}\text{Sr}_x\text{Co}_{1-y}\text{Nb}_y\text{O}_3$ solid solutions. The correlation between the long-range structure parameters and local electronic structure is discussed. The XANES sensitivity to the hole-doping effects, local lattice distortion and to an overlapping mixture of low and high or intermediate spin states of Co^{3+} and Co^{4+} ions in these cobaltites is also considered.

2. Experimental procedure

Single-phase polycrystalline $\text{La}_{1-x}\text{Sr}_x\text{Co}_{1-y}\text{Nb}_y\text{O}_3$ has been prepared from a mixture of simple oxides and carbonates by solid state reaction at a temperature of 1770 K in air. At temperature lower than 1720 K, the system consisted of two perovskite phases with a structure close to LaCoO_3 and $\text{Sr}(\text{Co}_{0.5}\text{Nb}_{0.5})\text{O}_3$.

The neutron powder diffraction experiments were carried out using the fine resolution neutron diffractometer E9 at the BER-II reactor in Hahn Meitner Institute [6]. Data were collected at 290 K over the range $4^\circ \leq 2\theta \leq 156^\circ$ at the wavelength $\lambda = 1.7973 \text{ \AA}$. The neutron powder diffraction data were analyzed by the Rietveld method using the FullProf program [7].

X-ray powder diffraction experimental data were collected at Siberian Synchrotron Radiation Center (SSRC) using high-resolution powder diffractometer at room temperature. Monochromatization of primary synchrotron radiation beam was performed by Si(111) monochromator. Radiation wavelength was 1.5398 Å. Diffractometer is equipped by Ge(111) crystal analyzer on the diffracted beam providing extremely high instrumental resolution and accuracy of data. The data were analyzed using the FullProf program [7].

The Co K-edge ($E_K = 7709 \text{ eV}$) XANES spectra were measured at the EXAFS station of SSRC. The storage ring VEPP-3 with electron beam energy of 2 GeV and an average stored current of 80 mA was used as the radiation source. The X-ray energy was monochromatized with a channel-cut Si(111) crystal monochromator. The Co K-edge XANES spectra were recorded in transmission mode, using two ionization chambers filled with argon gas as detectors. The energy resolution was about 1.0 eV. The samples were prepared as pellets with a thickness to obtain the value of the absorption edge jump equal to 1.0–1.3.

Co $L_{2,3}$ -edges ($E_{L_{2,3}} = 796$ and 783 eV) XAS measurements were performed on the Russian–German beamline [8] at the BESSY II in Berlin. The X-ray energy was monochromatized with a channel-cut Si(111) crystal monochromator. The Co $L_{2,3}$ -edges XANES spectra were recorded in total electron yield (TEY) mode. The energy

resolution was about 0.15 eV. All the measurements were carried out at 290 K.

The XANES data were analyzed by the WINXAS code [9] in the range 7690–7730 eV. The data were normalized by setting a point located at about 200 eV above the edge to unity.

3. Experimental results and analysis

3.1. X-ray and neutron diffraction results

Preliminary study of crystal structure of $\text{La}_{1-x}\text{Sr}_x\text{Co}_{1-x/2}\text{Nb}_{x/2}\text{O}_3$ compounds was performed using X-ray diffraction data. All observed Bragg peaks were indexed in the rhombohedral R-3c space group in hexagonal axes. There were no impurities according to these data. The result of the neutron diffraction patterns refinement is in agreement with the X-ray analysis.

The room-temperature data for $\text{La}_{1-x}\text{Sr}_x\text{Co}_{1-y}\text{Nb}_y\text{O}_3$ were analyzed by the Rietveld refinement method, and the result for $\text{La}_{0.5}\text{Sr}_{0.5}\text{Co}_{0.9}\text{Nb}_{0.1}\text{O}_3$ is shown in Fig. 1. Some structural parameters calculated from the neutron diffraction patterns are given in Table 1.

3.2. X-ray absorption results

The Co K-edge XANES consists of the small pre-edge peak and the main absorption edge with a fine structure above it (Fig. 2). The second derivatives of the spectra in the region of the pre-edge peak are shown for LaCoO_3 , $\text{La}_{0.8}\text{Sr}_{0.2}\text{Co}_{1-y}\text{Nb}_y\text{O}_3$ ($y = 0.0; 0.1$) and $\text{La}_{0.5}\text{Sr}_{0.5}\text{Co}_{1-y}\text{Nb}_y\text{O}_3$ ($y = 0.0; 0.1; 0.25$) in Figs. 3–5, respectively.

Substitution of Co by Nb in $\text{La}_{1-x}\text{Sr}_x\text{Co}_{1-y}\text{Nb}_y\text{O}_3$ ($y = 0.0; 0.1; 0.2; 0.25$) leads to a decrease of the intensity of the pre-edge peak and to a gradual increase of its splitting into two peaks, which correspond to the e_g and t_{2g}

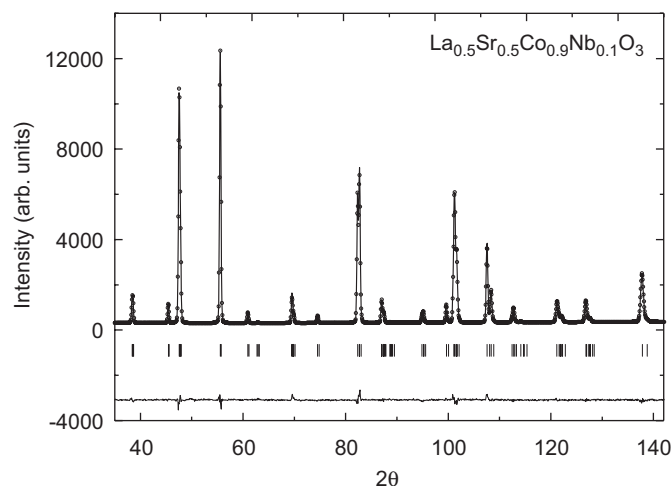


Fig. 1. Neutron diffraction pattern of $\text{La}_{0.5}\text{Sr}_{0.5}\text{Co}_{0.9}\text{Nb}_{0.1}\text{O}_3$: experimental curve (continuous line), refinement points (open circles), and their difference (continuous line below). Ticks show the predicted 2θ positions for the Bragg peaks.

Table 1
Structural parameters for $\text{La}_{1-x}\text{Sr}_x\text{Co}_{1-y}\text{Nb}_y\text{O}_3$ at room temperature

	$x = 0.0, y = 0.0$	$x = 0.2, y = 0.0$	$x = 0.2, y = 0.1$	$x = 0.5, y = 0.0$	$x = 0.5, y = 0.075$	$x = 0.5, y = 0.1$	$x = 0.5, y = 0.25$
a_h (Å)	5.4512 (2)	5.4430 (2)	5.4631 (3)	5.4219 (4)	5.4506 (5)	5.45756 (7)	5.5081 (6)
c_h (Å)	13.0152 (5)	13.1692 (3)	13.21745 (9)	13.2137 (4)	13.2800 (2)	13.29255 (8)	13.4147 (2)
V (Å ³)	111.962	337.8888	341.642 (1)	336.409 (2)	341.680 (2)	342.875 (2)	352.469 (2)
x [O]	0.4531 (7)	0.4588 (4)	0.4571 (2)	0.4741 (3)	0.47179 (17)	0.47013 (18)	0.4641 (3)
$d_{\text{Co-O}}$ (Å)	1.9225 (3)	1.9296 (4)	1.9378 (1)	1.9188 (1)	1.92980 (7)	1.93279 (8)	1.9537 (1)
$\theta_{\text{Co-O-Co}}$ (deg)	165.115	166.653 (8)	166.107 (6)	171.606 (5)	170.860 (3)	170.323 (3)	168.382 (7)
R_{wp} (%)	6.31	7.57	7.44	7.87	5.06	5.07	7.69
R_p (%)	4.59	6.08	6.61	5.79	3.82	3.95	6.28
R_f (%)	5.79	5.56	4.43	4.33	4.23	3.27	6.38
R_{exp} (%)	4.26	4.50	4.87	5.43	3.82	3.92	5.41

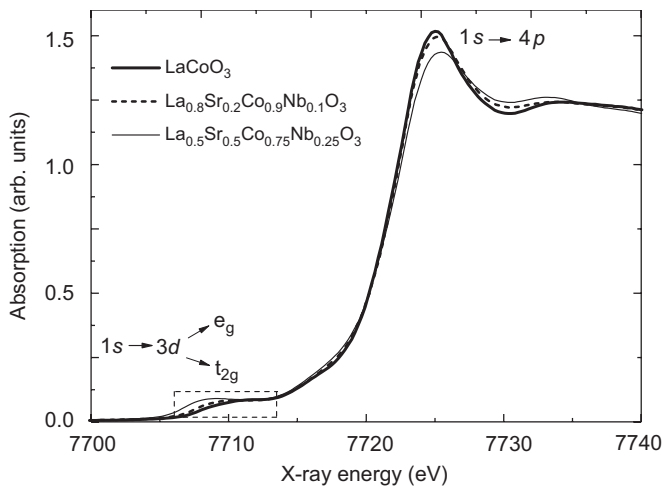


Fig. 2. XANES spectra at the Co K-edge for the LaCoO_3 , $\text{La}_{0.8}\text{Sr}_{0.2}\text{Co}_{0.9}\text{Nb}_{0.1}\text{O}_3$, and $\text{La}_{0.5}\text{Sr}_{0.5}\text{Co}_{0.75}\text{Nb}_{0.25}\text{O}_3$.

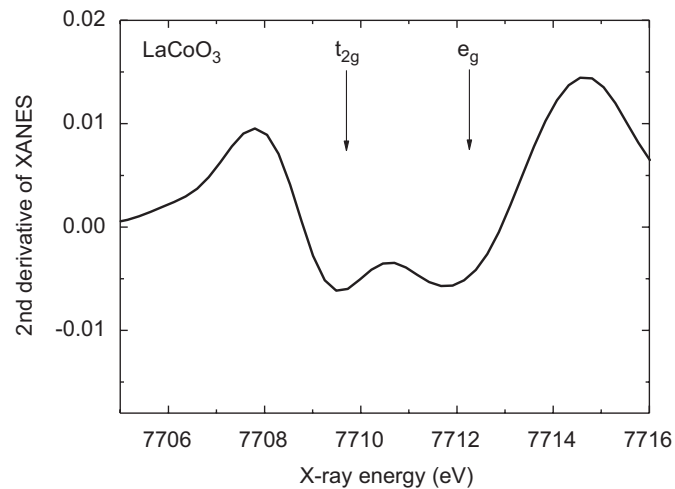


Fig. 3. The second derivative of the Co K-edge XANES spectra for LaCoO_3 .

bands (see Figs. 4 and 5). A slight decrease of these bands intensity in comparison with $\text{La}_{0.8}\text{Sr}_{0.2}\text{CoO}_3$ and $\text{La}_{0.5}\text{Sr}_{0.5}\text{CoO}_3$ is caused by the partial substitution of cobalt for Nb. The growth of the e_g and t_{2g} bands splitting at the substitution of cobalt for Nb could indicate a decrease of

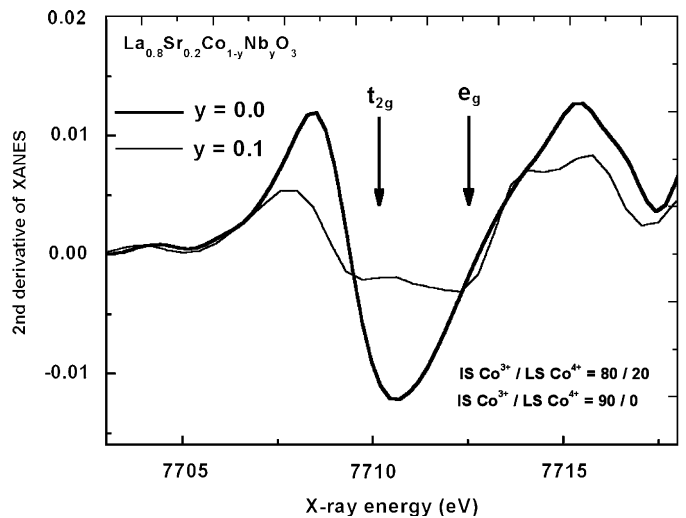


Fig. 4. The second derivative of the Co K-edge XANES spectra for $\text{La}_{0.8}\text{Sr}_{0.2}\text{Co}_{1-y}\text{Nb}_y\text{O}_3$ ($y = 0.0; 0.1$).

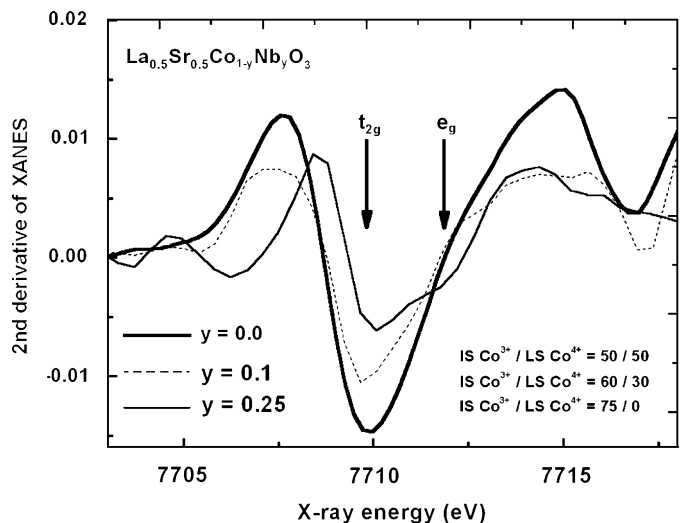


Fig. 5. The second derivative of the Co K-edge XANES spectra for $\text{La}_{0.5}\text{Sr}_{0.5}\text{Co}_{1-y}\text{Nb}_y\text{O}_3$ ($y = 0.0; 0.1; 0.25$).

low spin Co^{4+} [3] contribution and an increase of intermediate or high spin Co^{3+} influence similar to the results obtained for LaCoO_3 [10,11].

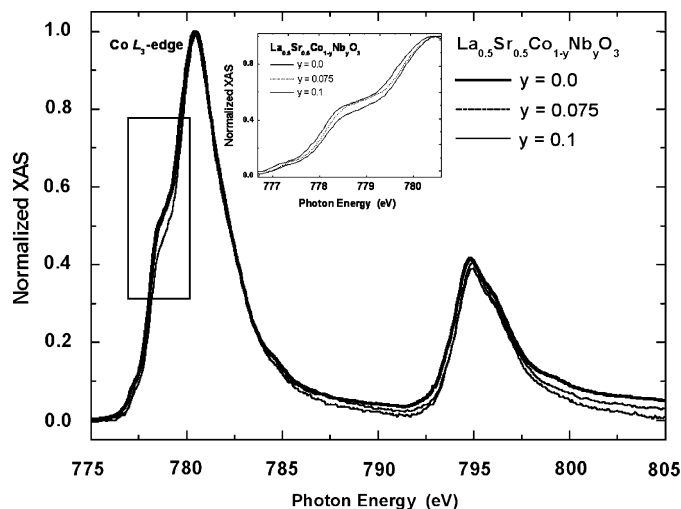


Fig. 6. Normalized XAS at the Co $L_{2,3}$ -edges of $\text{La}_{0.5}\text{Sr}_{0.5}\text{Co}_{1-y}\text{Nb}_y\text{O}_3$ ($y = 0.0; 0.075; 0.1$); the plot in the inset shows the region of the shoulder at 778.5 eV.

The doping dependence of the Co $L_{2,3}$ -edges recorded at room temperature for the series $\text{La}_{0.5}\text{Sr}_{0.5}\text{Co}_{1-y}\text{Nb}_y\text{O}_3$ ($y = 0.0; 0.075; 0.1$) is shown in Fig. 6. The spectra correspond to transitions from Co 2p states to unoccupied Co 3d states mixed with O 2p states. Upon Nb doping, a change in the shape of the shoulder at the Co L_3 -edge is observed (Fig. 6, inset), indicating that new electronic states appear below the Fermi level.

The obtained results suggest that a correlation between structural parameters, as the Co–O distance and Co–O–Co angle from neutron diffraction data (Table 1), and the local electronic structure of Co ions, probed by XANES,

is observed. An introduction of Nb ions leads to an increase of the average Co–O distance and a decrease of the Co–O–Co angle, that influences the Co–O interaction and appears in XANES as a broadening of the Co 3d-band.

Acknowledgment

This work was supported by Russian Foundation for Basic Research (Grant no. 06-02-81038) and by Belorussian Foundation for Basic Research (Grant no. F06R-134).

References

- [1] P.M. Raccach, J.B. Goodenough, Phys. Rev. 155 (1967) 932.
- [2] G. Briceño, H. Chang, X. Sun, P.G. Schuit, X.-I. Xiang, Science 270 (1995) 273.
- [3] M.A. Senaris-Rodríguez, J.B. Goodenough, J. Solid State Chem. 118 (1995) 323.
- [4] I.O. Troyanchuk, D.V. Karpinsky, R. Szymczak, Phys. Stat. Sol. b 242 (2005) 49.
- [5] D. Tobben, N. Stüßer, K. Knorr, G. Lampert, Mater. Sci. Forum 378–381 (2001) 288.
- [6] J.L. Rodríguez-Carvajal, Physica B 55 (1992) 192.
- [7] A.S. Vinogradov, S.I. Fedoseenko, D.V. Vyalikh, S.L. Molodtsov, V.K. Adamchuk, C. Laubschat, G. Kaindl, Nucl. Instr. and Meth. Phys. Res. A 505 (2003) 718.
- [8] T. Ressler, J. Synchrotron Radiat. 5 (1998) 118.
- [9] R.H. Potze, G.A. Sawatzky, M. Abbate, Phys. Rev. B 51 (1995) 11501.
- [10] O. Haas, R.P.W.J. Struis, J.M. McBreen, J. Solid State Chem. 177 (2004) 1000.
- [11] V. Efimov, E. Efimova, D.I. Kochubey, V.V. Kriventsov, A. Kuzmin, V. Sikolenko, A.N. Shmakov, S.I. Tiutiunnikov, I.O. Troyanchuk, Surface (Russia) 6 (2006) 23.